TELKOMNIKA Telecommunication, Computing, Electronics and Control
Vol. 18, No. 1, February 2020, pp. 301~310
ISSN: 1693-6930, accredited First Grade by Kemenristekdikti, Decree No: 21/E/KPT/2018
DOI: 10.12928/TELKOMNIKA.v18i1.13130

Investigation on EM radiations from interconnects in integrated circuits

Lounas Belhimer, Arezki Benfdila, Ahcene Lakhlef
Micro and Nanoelectronics Research Group, Faculty of Electrical Engineering and Computer Sciences,
University Mouloud Mammeri, Tizi-Ouzou, Algeria

Article Info

Article history:

Received May 22, 2019
Revised Jul 2, 2019
Accepted Jul 18, 2019

Keywords:

Capacitance
Electromagnetic
Finite element method
Interconnect
Multiconductor
Radiations
Transmission lines

ABSTRACT

Characterization and estimation of interconnections behavior in integrated circuits design before the implementation phase is of paramount importance. This behavior seen as microstrip antennas gets complex as the internal signal (square or sine waves) frequencies increase. Thus, they become the preferred path for the propagation of electromagnetic disturbances. In this work we have worked out the numerical modeling of the electromagnetic interactions characterizing the electromagnetic compatibility in the microstrip transmission lines. The effect of these electromagnetic interactions in different structures topologies are studied through the analysis of the influence of the supply signals frequency and structures. The spacing between transmission line tracks and the number of tracks superposition is modeled. The evolution and variation of the scheme parameters in the frequency domain are determined. The transmission lines are considered parallel of equal spacing and superposed tracks of equal spacing and thickness. The capacitance and inductance matrices are computed and discussed. The results are found to comply with current research outcomes.

Corresponding Author:

Arezki Benfdila,
Micro and Nanoelectronics Research Group,
Faculty of Electrical Engineering and Computer Sciences,
University Mouloud Mammeri,
Tizi-Ouzou, Algeria.
Email: benfdila@ummto.dz

1. INTRODUCTION

Nowadays, integrated circuits electromagnetic susceptibility threshold gets lower due to the integration densities increasing and higher levels of metallization. This increased vulnerability results from their size shrinking, supply voltage and the regular increase in their operation frequencies [1, 2]. Gigahertz frequencies are particularly harmful for these electronic systems because their wavelengths are likely to generate resonance phenomena on the integrated circuits tracks, thus increasing the system disturbance risks [3-5].

As microelectronics technology progresses, manufacturers are continually striving to build higher density electronic systems integration. This evolution is characterized by a regular device shrinking and a multilevel integration [6]. This led to acomplex interconnection circuitry consisting of parallel planes of equidistant transmission lines. Today this becomes a complex problem faced in the improvement of the integrated circuits performances [7]. When designing and implementing an electronic system, the possible electromagnetic interactions should be taken into account and methods should be provided to reduce their influence sufficiently, so as to ensure safe operation in most cases [8, 9].

Ensuring electromagnetic compatibility at the integrated circuit level implies effective reduction of noise sources and disturbances origins. The modeling of these facts becomes mandatory to ensure a predictive approach to the risks of EM-induced disruption [10, 11]. This requires specific tools, models and EMC knowledge [12, 13]. The designer of integrated circuits should consider the capacitances and inductances that were not considered in earlier times, because of the interconnection's lengths and the higher operating frequencies [14, 15]. The study of electromagnetic radiation in an integrated circuit requires knowledge of the electromagnetic fields in this device and therefore the flux values [16]. The calculation of the magnetic field requires a resolution of Maxwell equations. This is achieved by several computational methods, such as the Method of Finite Element, finite differences and the method of moments [17, 18].

In order to further improve the integrated circuit several calculation models have been proposed to estimate the behavior of the interconnection's lines, as it was presented in [19. 20]. And may researchers have calculated and simulated the electromagnetic problem [21-23]. In this paper we have used the finite element method to determine the radiation and the coupling between its interconnection tracks in order to integrate all the line fields surrounding an interconnect line. We have organized the paper as follows: in the seconde part we have given the definition of the finite element method, in the third part a mathematical model has been developped to minimize electromagnetic disturbance on circuits interconnects, and in the fifth part the circuits interconnect has been simulated with defferents parameters in order to achieve an interconnection structure with less energy losses.

2. THE FINITE ELEMENT METHOD

The finite element approach is based on solving partial differential equations knowing the boundary conditions. This method was initially used for solving problems in the field of fracture mechanics and structural design (by mechanics). The method was first used for computing the electromagnetic field in the 1970s by P.P Silvester and M.V.K Chari. In most cases, it is integrated with C.A.O softwares and showed great advantage for the designers of physical systems [24].

The basic approach of the finite element method is to subdivide the field of study into finite numbers of subdomains called elements as show in Figure 1. The approximation of the unknown values is done for each element of the interpolation functions. This function is defined based on the geometry of the element that is chosen beforehand and fits with the nodes of this element with respect to the unknown values. This is called nodal interpolation [25].

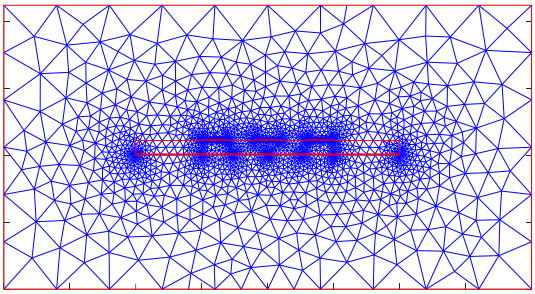

Figure 1. Mesh by finite element

3. THE MATHEMATICAL MODEL

In the following, we will be developing a mathematical model that governs electromagnetic compatibility problems of the magnetization conservation. Using the Maxwell equation, we can deduce the relation that links the magnetic induction to the magnetic vector potential as:

$$\vec{\nabla}.\vec{B} = 0 \Rightarrow \exists \vec{A}/\vec{B} = \vec{\nabla}\hat{}\vec{A} \quad (1)$$

introducing (1) into Maxwell Faraday equation we will have:

$$\vec{\nabla}\hat{}\left(\vec{E} + \frac{\partial \vec{A}}{\partial t}\right) = 0 \quad (2)$$

since the rotational of a gradient is null, we can deduce the existence of an electric scalar potential V, and then we write it as:

$$\exists V/\vec{E} + \frac{\partial \vec{A}}{\partial t} = -\overrightarrow{grad}V \quad (3)$$

we have:

$$\vec{E} = -\frac{\partial \vec{A}}{\partial t} - \overrightarrow{grad}V \quad (4)$$

replacing (4) in the expression of Ohm's law we get:

$$\vec{J} = \sigma\overrightarrow{grad}V - \sigma\frac{\partial \vec{A}}{\partial t} \quad (5)$$

we have

$$\overrightarrow{J_s} = \sigma\overrightarrow{grad}V \quad (6)$$

$\overrightarrow{J_s}$**:** current density of the excitation source

$$\vec{J} = \overrightarrow{J_s} - \sigma\frac{\partial \vec{A}}{\partial t} \quad (7)$$

by introducing the (1) in the relation of magnetic medium we get:

$$\vec{H} = \frac{\vec{\nabla}\wedge\vec{A}}{\mu} \quad (8)$$

replacing (8) in the Maxwell-Ampere equation and applying to it the rotational we will have:

$$\vec{\nabla}\wedge\left(\frac{\vec{\nabla}\wedge\vec{A}}{\mu}\right) = \overrightarrow{J_s} - \sigma\frac{\partial \vec{A}}{\partial t} + \frac{\partial \vec{D}}{\partial t} \quad (9)$$

taking into account the relation of a dielectric medium and replacing (4) in (9) we obtain the following set of equations:

$$\vec{\nabla}\wedge\left(\frac{\vec{\nabla}\wedge\vec{A}}{\mu}\right) = \overrightarrow{J_s} - \sigma\frac{\partial \vec{A}}{\partial t} + \varepsilon\frac{\partial \vec{E}}{\partial t} \quad (10)$$

$$\vec{\nabla}\wedge\left(\frac{\vec{\nabla}\wedge\vec{A}}{\mu}\right) = \overrightarrow{J_s} - \sigma\frac{\partial \vec{A}}{\partial t} + \varepsilon\frac{\partial}{\partial t}\left(-\frac{\partial \vec{A}}{\partial t} - \overrightarrow{grad}V\right) \quad (11)$$

$$\vec{\nabla}\wedge\left(\frac{\vec{\nabla}\wedge\vec{A}}{\mu}\right) = \overrightarrow{J_s} - \sigma\frac{\partial \vec{A}}{\partial t} + \varepsilon\frac{\partial^2 \vec{A}}{\partial t^2} - \overrightarrow{grad}\frac{\partial V}{\partial t} \quad (12)$$

it is known that:

$$\vec{\nabla}\wedge\vec{\nabla}\wedge\vec{A} = -\nabla^2\vec{A} + \overrightarrow{grad}\left(\vec{\nabla}.\overrightarrow{A}\right) \quad (13)$$

$$-\frac{1}{\mu}(\nabla^2\vec{A}) = \overrightarrow{J_s} - \sigma\frac{\partial \vec{A}}{\partial t} - \varepsilon\frac{\partial^2 \vec{A}}{\partial t^2} - \overrightarrow{grad}\left(\vec{\nabla}.\vec{A} + \mu\varepsilon\frac{\partial \vec{V}}{\partial t}\right) \quad (14)$$

to completely define the magnetic potential vector, one imposes the condition of Lorentz:

$$\vec{\nabla}.\vec{A} + \mu\varepsilon\frac{\partial \vec{V}}{\partial t} = 0 \quad (15)$$

Then (14) is simplified as given below:

$$-\frac{1}{\mu}\nabla^2\vec{A}+\sigma\frac{\partial\vec{A}}{\partial t}+\varepsilon\frac{\partial^2\vec{A}}{\partial t^2}=\vec{J_s} \quad (16)$$

we consider that the propagation is done in a Cartesian coordinates system along the z axis, and then the propagation equation of the magnetic vector potential will be:

$$-\frac{1}{\mu}\left[\frac{\partial^2 A_z}{\partial x^2}+\frac{\partial^2 A_z}{\partial y^2}\right]+\sigma\frac{\partial A_z}{\partial t}+\varepsilon\frac{\partial^2 A_z}{\partial t^2}=J_z \quad (17)$$

if we consider the sinusoidal harmonic regime this leads to:

$$-\frac{1}{\mu}\left[\frac{\partial^2 A_z}{\partial x^2}+\frac{\partial^2 A_z}{\partial y^2}\right]+(j\sigma\omega-\varepsilon\omega^2)A_z=J_z \quad (18)$$

$A_{z,\ Jz}$: are respectively the component of the magnetic vector potential and the current density source along the z axis. In the (18) characterizes the propagation of the magnetic vector potential. This latter will be considered in the following part of this work to model the electromagnetic interaction phenomena of the interconnections in an integrated circuit.

For solving the potential magnetic vector propagation equation, considering the finite element formulation, we have introduced the Galerkin method [14] defined in a Cartesian coordinate system. The propagation is considered according to the oz axis, by considering the phenomenon is governed by the equation:

$$-\frac{1}{\mu}\left[\frac{\partial^2 A_z}{\partial x^2}+\frac{\partial^2 A_z}{\partial y^2}\right]+(j\sigma\omega-\varepsilon\omega^2)A_z-J_z=0 \quad (19)$$

$$\iint_\Omega\left(\left(-\frac{1}{\mu}\left[\frac{\partial^2 A_z}{\partial x^2}+\frac{\partial^2 A_z}{\partial y^2}\right]+(j\sigma\omega-\varepsilon\omega^2)A_z\right)-J_z\right)\phi_i\,dx\,dy=0 \quad (20)$$

$$\iint_\Omega\left(-\frac{1}{\mu}\left[\frac{\partial^2 A_z}{\partial x^2}+\frac{\partial^2 A_z}{\partial y^2}\right]\right)\Phi_i\,dx\,dy+\iint_\Omega((j\sigma\omega-\varepsilon\omega^2)A_z)-\iint_\Omega J_z\Phi_i\,dx\,dy=0 \quad (21)$$

$$-\frac{1}{\mu}\iint_\Omega\vec{\nabla}\phi_i\vec{\nabla}A_z dxdy+\int_\Gamma\phi_i\frac{\partial A_z}{\partial n}d\Gamma+(j\sigma\omega-\varepsilon\omega^2)\iint_\Omega A_z\phi_i dxdy=\iint_\Omega J_z\phi_i dxdy \quad (22)$$

using the boundary Dirichlet conditions, this leads to:

$$\int_\Gamma\phi_i\frac{\partial A_z}{\partial n}d\Gamma=0 \quad (23)$$

$$-\frac{1}{\mu}\iint_\Omega\vec{\nabla}\phi_i\vec{\nabla}A_z dxdy+(j\sigma\omega-\varepsilon\omega^2)\iint_\Omega A_z\phi_i dxdy=\iint_\Omega J_z\phi_i dxdy \quad (24)$$

$$A=\sum_{j=1}^{N}\phi_j A_j \quad (25)$$

$$\sum_{j=1}^{N}\left[-\frac{1}{\mu}\iint_\Omega\vec{\nabla}\phi_i\vec{\nabla}\phi_j dxdy\right]A_j+(j\sigma\omega-\varepsilon\omega^2)\sum_{j=1}^{N}\left[\iint_\Omega\phi_i\phi_j dxdy\right]A_j=\iint_\Omega J_z\phi_i dxdy \quad (26)$$

for all mesh nodes, the following matrix system can be written:

$$[M][A]+(j\sigma\omega-\varepsilon\omega^2)[L][A]=[K] \quad (27)$$

$$M_{ij}=-\frac{1}{\mu}\iint_\Omega\vec{\nabla}\phi_i\,\vec{\nabla}\phi_j dxdy \quad (28)$$

$$L_{ij} = \iint_{\Omega} \phi_i \, \phi_j dxdy = \iint_{\Omega} \phi_i J_z dxdy \quad (29)$$

[A] and [K] are respectively the unknown vector and the excitation source vector
[M] and [L] are two matrices that depend on the mesh structure

4. PARAMETERS IDENTIFICATION OF THE EQUIVALENT CIRCUIT DIAGRAM

It is important for an integrated circuit designer to predict the behavior of his product in an electromagnetic interference environment. Interconnections are often victims of this electromagnetic pollution. This part consists of a numerical modeling of the electromagnetic interferences. We will analyze the influence of the frequency parameters of the supply signal and spacing between track and the permittivity of dielectric on the evolution of the parameters of the equivalent diagram. The interconnection lines can be modeled using their distributed constants, the equivalent diagrams are shown in Figure 2, it represents a track portion in the form of an electrical quadrupole that links the characteristics (i, v) of the position (z + dz) to that of position (z) at time (t).

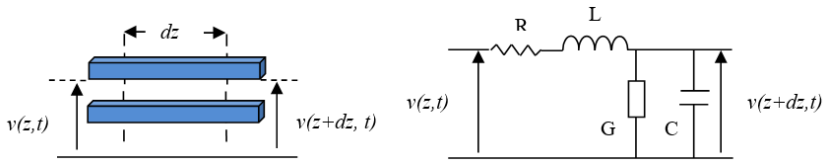

v(z,t):represents the voltage at position "z"
v(z+dz,t):represents the voltage at position "z+dz"

Figure 2. Equivalent circuit of a strip portion

The parameters of the equivalent diagram are: the equivalent inductance "L" per unit length, it characterizes the magnetic energy density stored in the medium, the equivalent capacitance "C" per unit length, it characterizes the density of dielectric energy stored in the substrate, the resistance series per unit length "R", it characterizes the losses by Joule effect, the parallel conductance per unit length "G", it characterizes the losses in the insulation. Joules losses were used to evaluate the linear resistance given by the following relation:

$$R = \frac{P_J}{I^2} \quad [\Omega/\mathrm{m}] \quad (30)$$

$$P_J = \iiint_v \frac{J^2}{\sigma} \, \mathrm{dv} \quad (31)$$

$$L = \frac{2^* W_{mag}}{I^2} \quad [\mathrm{H/m}] \quad (32)$$

to evaluate the inductance, the following magnetic energy should be used:

$$W_{mag} = \iiint_v \frac{1}{2} \mu_0 \mu_r |H|^2 dv \quad (33)$$

$$C = \frac{2^* W_{dielc}}{V^2} \quad [\mathrm{F/m}] \quad (34)$$

the dielectric energy is used to evaluate the linear capacitance:

$$W_{dielc} = \iiint_v \varepsilon_0 \varepsilon_r |E|^2 dv \quad (35)$$

to evaluate the conductance of the substrate, we will use a formula that includes the capacity:

$$G = C^* \omega^* \tan\delta \quad [\mathrm{S/m}] \quad (36)$$

tanδ: dissipation factor (dielectric loss angle)

To study the parameters of equivalent diagrams as a function of the supply frequency, the distance between the track and the permittivity, we have elaborated the flowshrt shown in Figure 3 which has been used to design our computation programs. At the start of our program as shown in Figure 3 we introduce geometry and physical characteristics from model to modeled. After having meshed the field of study, we will solve the partial differential equation at each mesh point and identify the parameters (R, L, C, and G) of the interconnection line for a given frequency and distance between tracks. Each time the frequency and the distance between tracks are incremented.

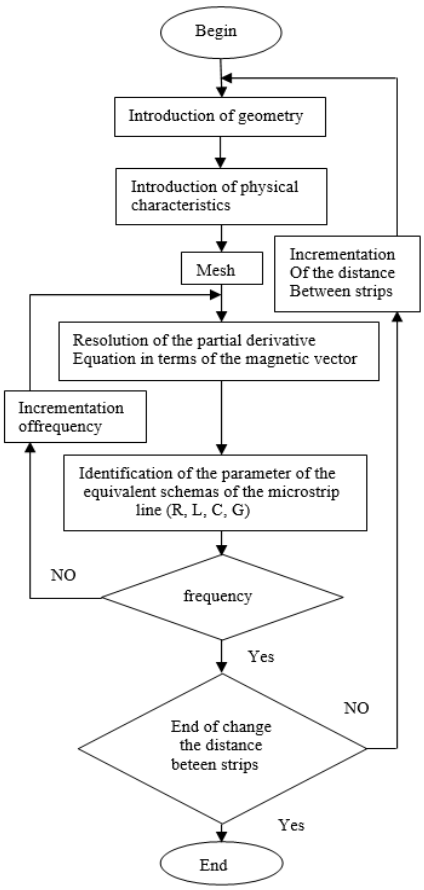

Figure 3. Flowchart used to study the parameters of the equivalent circuit as a function of supply frequency, the distance between the track and the permittivity

5. RESULTS AND DISCUSSION

5.1. Ground plane effect

In this part we will study the effect of ground plane on the impedance of the interconnects. We consider the structures in Figure 4, this microstrip coupled interconnect has the following geometrical parameters w = 2 μm, S = 5 nm, h = 1 μm, H = 3 μm, ε = 3.9 In this case we note a significant increase in the capacity towards the mass which is due to the lines of fields which refocus towards the mass as show in Figure 5.

5.2. Influence of the frequency

In our analysis we based our system on a two parallel transmission lines. This corresponds to a 2 lines of an n line internal integrated circuit bus. The three-line configuration is used to discuss the interdependance of the two-line Transmission lines. This microstrip coupled interconnects have the following geometrical parameters: w = 2 μm, S = 5 nm, h = 1 μm, H = 3 μm, ε = 3.9. The three microstrip lines as shown in Figure 6 are equidistance and mounted on a oxide grown on silicon substrate. We simulated and modeled the interconnect capacitance in different situation. The Figures 7 show inductance and resistance versus frequency.The increase in resistance is due to the skin effect which causes the distribution of the current density in the section of the track to become non-uniform with the increase of the frequency

and the current that travels the track will tend to circulate on this periphery in a section defined by a thickness called "skin thickness". Therefore, the active section of the track decreases and therefore the resistance increases.

We also note that the inductance of the track decreases as the frequency increases as shown in Figure 8. According to the relation of the inductance it is understood that, as regards the internal volume of the conductor, the contribution to the integral of the magnetic energy is even smaller than the frequency is large. It is found that the capacity increases with the increase of the frequency, this is explained as much as the frequency is more important the dielectric energy will tend increased consequently the capacity increases.

The increase in conductance as show in Figure 9 is due to the increase in capacity, According to the equation of conductance. The obtained results well motivate the effect of the electromagnetic interactions on the electrical parameters of the interconnects, notably the impedance which has known an increase compared to that obtained in the absence of the electromagnetic interactions as show in Figure 10.

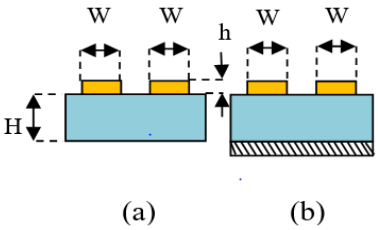

Figure 4. Microstrip coupled interconnect: (a) without ground plane, (b) with ground plane

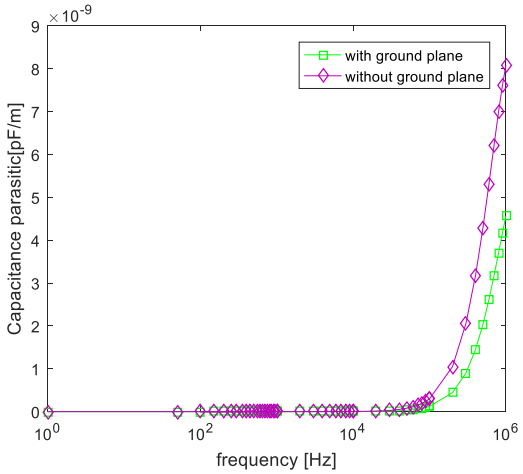

Figure 5. Parasitic capacitance versus frequency

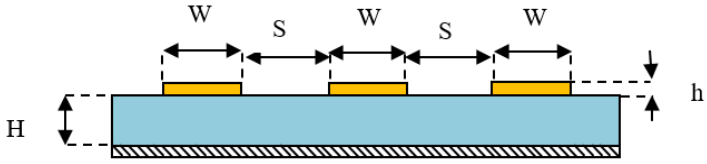

Figure 6. Symmetric microstrip coupled interconnects

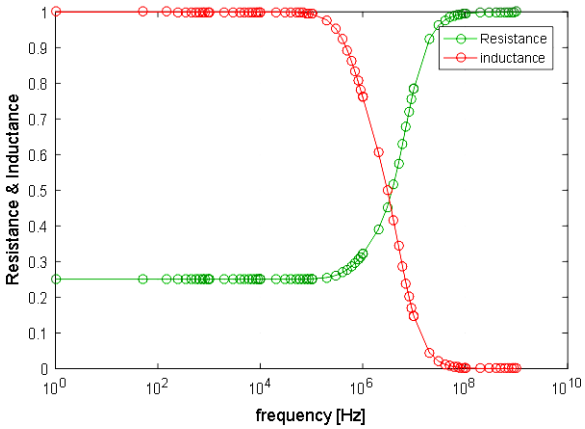

Figure 7. Inductance and resistance versus frequency

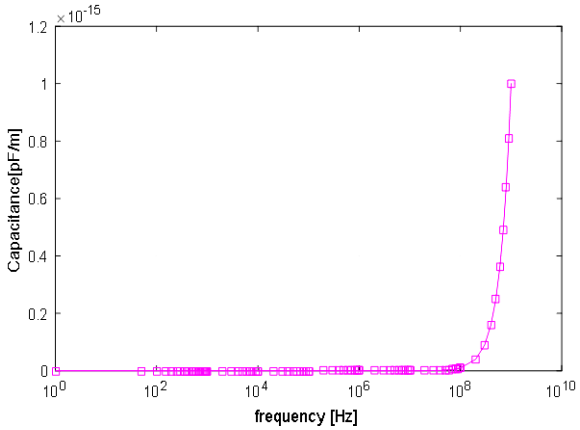

Figure 8. Capacitance versus frequency

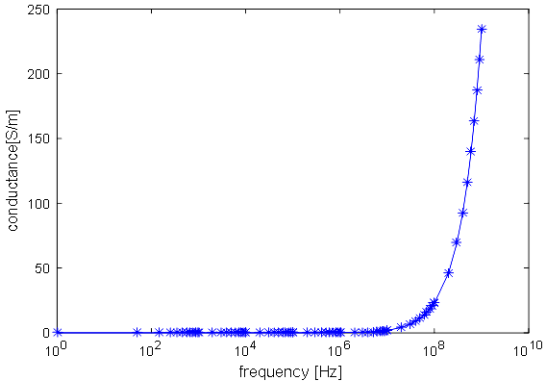

Figure 9. Conductance versus frequency

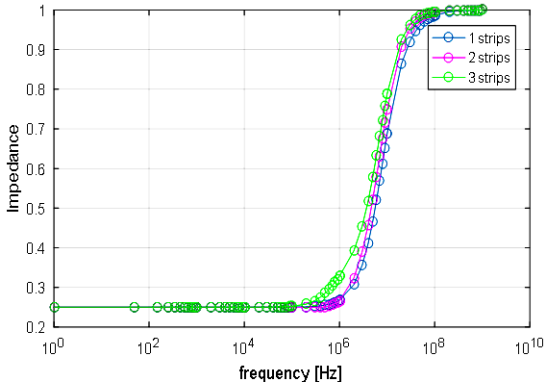

Figure 10. Summary and data comparison

5.3. Influence of the dielectric permittivity

We varied the dielectric permittivity and the frequency is fixed we calculate the new values of the parasitic capacitances. The permittivity is directly related to the dielectric energy so by increasing the permittivity the dielectric energy also increases consequently the parasitic capacitance increases as show in Figure 11 and Figure 12.

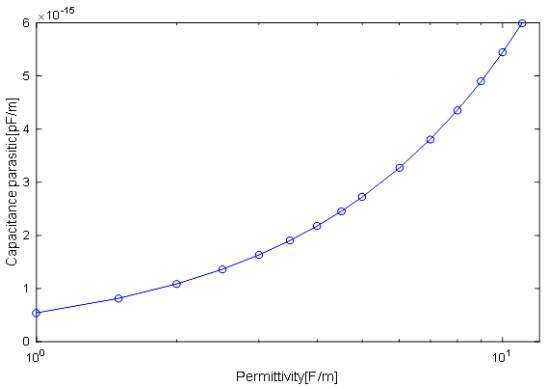

Figure 11. Parasitic capacitance versus Permittivity

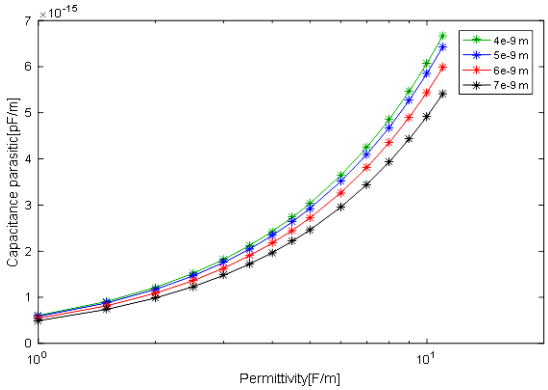

Figure 12. Parasitic capacitance versus permittivity for different S value

5.4. Influence of the distance inter tracks

For different values of "S" (the distance between two interconnection tracks), it sets the working frequency is 1 gigahetrz we calculate the value of the capacity and inductance per unit length. As show in the Figure 13 and Figure 14, the capacity decreases with the distance between tracks, this evolution can be explained by the fact that we associate the increase in the distance between tracks, in order to locate an optimal layer thickness corresponding to the thickness for which the spurious capacitance track ratio is the lowest.

5.5. Modeling of crosstalk

Any unwanted voltage or current and created by coupling between two tracks of an interconnection network is considered to be crosstalk. In what follows, we propose to model the tension induced by a track on another track that is adjacent to it. For that we consider the precinct structure. According to the law of faraday, the coupling in magnetic field induces a voltage V_{in} directly related to the variations of the magnetic flux Φ which crosses the conductor of section "s" and it is written as follows:

$$V_{in} = -\frac{d\phi}{dt} \tag{37}$$

$$\vec{\phi} = \iint_s \vec{B}\overrightarrow{dS} \tag{38}$$

$$\vec{B} = rot\vec{A} \quad (39)$$

In this part always considers the Figure 6, but this time with the following dimensions: w = 20 µm, S = 20 µm, h = 5 µm, H = 40 µm, ε = 3.9. Considering a supply voltage of 2 V, with a track which has a length of 0.5 m, we get the following simulation results in Figure 15 and Figure 16. The Figure 15 represents the results of simulation of the crosstalk as a function of the frequency of the signal compared with that obtained in [4]. We see that there is some agreement between the two results, and a relationship of proportionality links the crosstalk and the frequency. We see that from the frequency 10 Hz the voltage drop begins to be felt. So, the signal injected at the beginning of the track undergoes attenuation due to the effects of high frequencies and electromagnetic interactions. Figure 16 represents the simulation of the voltage drop in the interconnection line for frequencies given as a function of the distance between tracks, it's noted that the voltage drop decreases with the increase in the distance between track and it increases with increased frequency

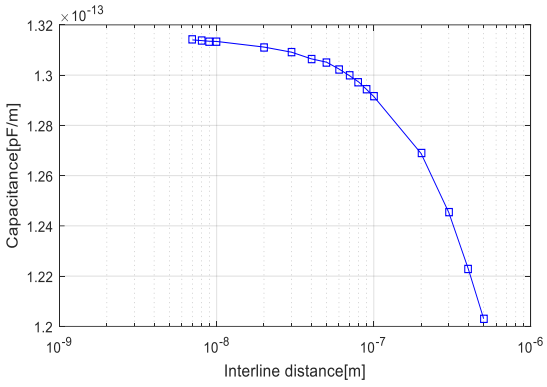

Figure 13. Parasitic capacitance versus inter line distance

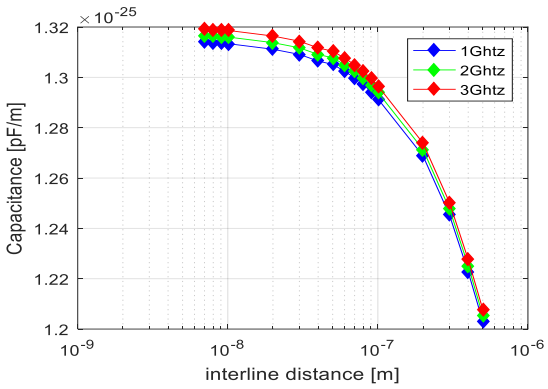

Figure 14. Parasitic capacitance versus inter line distance for different frequency

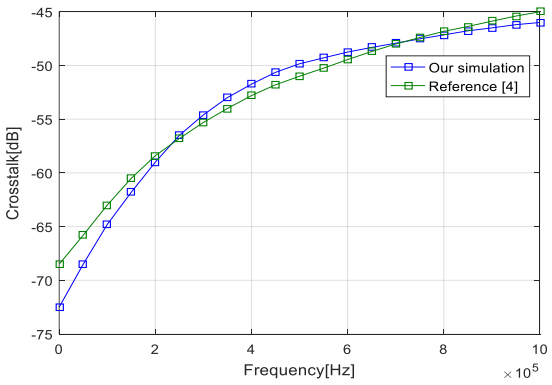

Figure 15. Crosstalk versus frequency

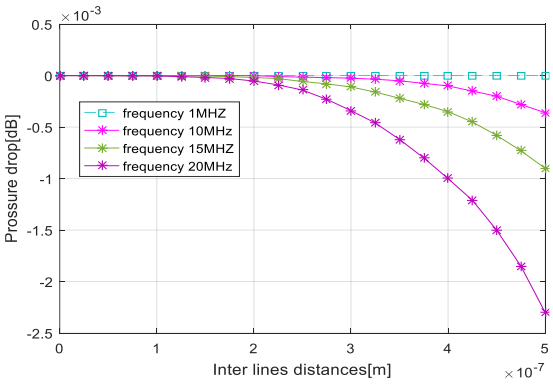

Figure 16. Pressure drop versus interline distance

6. CONCLUSION

The main conclusions are drawn for the study of the influence of dielectric width and permittivity. The transmission line length and geometry was also studied and the impedance per unit length is treated in order to estimate the losses and define the limit amplitude of the digital signal in use. We demonstrated that the capacitance and resistance increase with increasing frequency but the inductance decrease and by increasing the permittivity or the distance between tracks the parasitic capacitance decrease. Obtained literature results and with our simulations data, demonstrated that the crosstalk as a function of the frequency of the signal. Through these results, we can estimate the best materials for the best circuits interconnect geometry to ensure the best possible performance. The results are found to comply with literature and encouraging for further investigations on dielectric separation.

REFERENCES

[1] E. Sicard, W. Jian-fei, L. J. Cheng. "Signal intergrity and EMC performance enhancement using 3D Integrated Circuits-A Case Study," *9th International Workshop on Electromagnetic Compatibility of Integrated Circuits (EMC Compo)*, Nara, Japan, pp. 10-14, 15-18 December 2013.

[2] B. Zhu, J. Lu, M. Zhu. "Computational Electromagnetics for EMC Problems of Integrated Circuits," *10th International Symposium on Electromagnetic Compatibility*, York, UK, pp. 717-723, 26-30 September 2011.

[3] Mathias Magdovwski, SergyeKochetov and Marcon Leone "Modeling the Skin Effect in the Time Domain for Simulation of Circuit Interconnect," *IEEE-International Symposium on Electromagnetic Compatibility (EMC)* Europe, 2008.

[4] H. Ymeri, B. Nauwelaers, K. Maex, Vandenber, and D. De Roest, and Vandenber, "New analytic expression for mutual inductance and resistance of coupled interconnects on lossy silicon substrate," *2001 Topical Meeting on Silicon Monolithic Integrated Circuits in RF Systems. Digest of Papers*, pp. 7803-7129, September 2001.

[5] M. ramdani, E. Sicard, A. boyer, S. Ben Dhia, J. J. Walen, T. H. Hubing, M. Coenen, O. Wada "The electromagnetic compatibility of integrated circuits-past, present, future," *IEEE transaction on Electromagnetic compatibility*, vol. 51, no. 1, pp. 78-100, Februry 2009.

[6] H. N. Lin, C. W. Kuo, J. L. Chang, C. K. Chen. "Statistical Analysis of EMI Noise Measurement for Flash Memory," *8th Workshop on Electromagnetic Compatibility of Integrated Circuits*, Dubrovnik, Croatia, pp. 245-250, 6-9 November 2011.

[7] M. Kachout, J. Belhadj Tahar and F. Choubani, "Modeling of microstrip and PCB traces to enhance crosstalk reduction," *2010 IEEE Region 8 International Conference on Computational Technologies in Electrical and Electronics Engineering (SIBIRCON)*, Irkutsk Listvyanka, Russia, pp. 594-597, 11-15 July, 2010.

[8] Raouf Lawrence Khan and George I. Costache "Finite Elements Method Applied to Modeling Crosstalk Problems on Printed Circuit Boards," *IEEE transactions on Electromagnic Compatibility*, vol. 31, no. 1, pp. 5-15, February 1989.

[9] F. Medina and M. Horno, "Capacitance and inductance matrices for multistrip structures in multilayered anisotropic," *IEEE Transmission on microwave theory and techniques*, vol. 35, no.11, pp. 1002-1008, November 1987.

[10] J. Guo, F. Rachidi, S. V. Tkachenko, Y. Z. Xie, "Calculation of High-Frequency Electromagnetic Field Coupling to Overhead Transmission Line Above a Lossy Ground and Terminated with a Nonlinear Load," *IEEE Transmission on Antenna and Propagation*, vol. 67, no 6, pp. 4119-4132, June 2019.

[11] J. Guo, Y. Z. Xie, F. Rachidi, "Modeling of EMP Coupling to Lossless MTLs in Time Domain Based on Analytical Gauss-Seidel Iteration Technique," *IEEE Internationat Symposium on Electromagnetic Compatibility and IEEE Asia-Pacific Symposium on Electromagnetic Compatibility*, pp. 897-902, 2018.

[12] E. Sicard and A. Boyer, "Enhancing Engineers in EMC of Integrated Circuits," *EMC Compo 2011 - 8th workshop on Electromagnetic Compatibility on integrated Circuits*, Dubrovnik, Croatia, 6-9 November 2011.

[13] Y. Bacher, N. Froideveaux, P. Dupre, H. Braquet, G. Jacquemod, "Resonance Analysis for EMC Improvement in Integrated Circuits," *10th International Workshop on the Electromagnetic Compatibility of Integrated Circuits*, pp. 56-60, November 2015.

[14] M. S. Ullah and M. H. Chowdhury, "Analytical Models of High-Speed RLC Interconnect Delay for Complex and Real Poles," *IEEE Transaction on very large scale integration systems*, vol. 25, no. 6, pp.1831-1841, June 2017.

[15] R. Ianconescu, V. Vulfin, "Free Space TEM Transmission Lines Radiation Losses," [Online], Available: http://vixra.org/abs/1609.0420, 2016.

[16] A. Boyer, E. Sicard and S. Ben Dhia, "IC-EMC, a Demonstration Freware for Predicing Electromagnetic Compatibility Integrated Circuits," *19th International Zurich Symposium on Electromagnetic Compatibility*, May 2008.

[17] Yaowu Liu, Kang LAn and Kenneth K. Mei, "Capacitance Extraction for Electrostatic Multiconductor Problems by On-Surface MEI," *IEEE transactions on advanced packaging*, vol. 23, no. 3, pp. 1521-3323, August 2000.

[18] J. Guo, Y. Z. Xie, "An Efficient Model of Transient Electromagnetic Field Coupling to Multiconductor Transmission Lines Based on Analytical Iteractive Technique in Time Domain," *IEEE transactions on Microwave Theory and techniques*, vol. 66, no. 6. pp. 2663-2673, 2018.

[19] M. S. Ullah and M. H. Chowdhury, "A new pole delay model for RLC interconnect using second order approximation," *IEEE 57th International Midwest Symposium on Circuits and Systems*, pp.238-241, August 2014.

[20] V. R. Kumar, M. K. Majumder, A. Alam, N. R. Kukkam and B. K. Kaushik, "Stability and delay analysis of multi-layered GNR and mlti-walled CNT interconnects," *J. Comput. Electron*, vol. 14, no. 2, pp. 611-618, June 2015.

[21] B. Nouri, M. S. Nakhla, R. Achar, "Efficient Simulation of Nonlinear Transmission Lines via Model-Order Reduction," *IEEE Transactions on Microwave Theory and Thechniques*, vol. 65, no. 3, pp. 673-983, March 2017.

[22] H. Xue, A. Ametani, J. Mahseredjan, Y. Baba, F. Rachidi, I. Kocar, "Transnsient Responses of Overhead Cables Due to Mode Transition in High Frequency," *IEEE Transactions on Electromagnetic Compatibility*, vol. 60, no. 3, pp. 785-794, June 2018.

[23] G. Lugrin, S. V. Tkachenko, F. Rachidi, M. Rubintein, R. Cherkaoui, "High-frequency Electromagnetic Coupling to Multiconductor Transmission Lines of Finites Length," *IEEE Transactions on Electromagnetic Compatibility*, vol. 57, no. 6, pp. 1714-1723, December 2015.

[24] Gouri Dhatt and Gilbert Touzot Emmanuel Le Francois "Finite Element Method," Edition Lavoisier, 2005.

[25] Gouri Dhatt, Jean-Luis Batoz, "Modeling of structures widh finite element," Hermès Edition, Paris, 1990, 1995.